Electron and positron scattering from perfluorocyclobutane (c-C_4F_8) molecules

C. Makochekanwa,[1,2] O. Sueoka,[3] M. Kimura,[1] M. Kitajima,[2] and H. Tanaka[2]
[1]*Graduate School of Sciences, Kyushu University, Fukuoka 812-8581, Japan*
[2]*Physics Department, Sofia University, Chiyoda-ku, Tokyo 102-8554, Japan*
[3]*Department of Applied Science, Yamaguchi University, Ube 755-8611, Japan*
(Received 27 September 2004; published 24 March 2005)

Total cross sections (TCSs) are experimentally investigated for 0.8–600-eV electron and 0.7–600-eV positron scattering from c-C_4F_8 molecules using a linear transmission time-of-flight method, and a comparative study of the results is carried out in this paper. Electron-scattering differential cross sections (DCS) measurements carried out for energies 1.5–100 eV are used for a combined TCS and DCS discussion. These DCS results help to offer a better understanding of some of the structures observed in the TCSs. Fingerprints of a low-energy resonance, consistent with large electron attachment cross sections near 0 eV, have been observed below 2 eV where TCSs show a continually rising trend. Another resonance peak at ~8.5 eV, attributed to dissociative electron attachment with the production of fragmented ions, and a broader one at 16–40 eV, have also been observed. Except for the pronounced shoulder at ~40 eV, there is good qualitative agreement between the TCS result and the integrated cross-section results. Although electron TCSs are found to be generally larger than positron TCSs in the 3–120-eV ranges, these two TCSs, however, show a tendency towards merging above 120 eV.

DOI: 10.1103/PhysRevA.71.032717 PACS number(s): 34.80.Bm, 34.80.Dp, 36.10.Dr

I. INTRODUCTION

It has been known for a while that collisions of electrons with fluorocarbons are a primary step in plasma-processing chemistry and may also play a role in the chemistry of the freon-contaminated atmosphere. Besides plasma processing, these gases are also essential for other nanotechnologies. Perfluorocyclobutane (c-C_4F_8) molecules are a plasma processing gas employed in the plasma etching of semiconductors. Its CF_2 radicals have especially been used in the selective etching of SiO_2 [1,2]. These CF_2 radicals are also formed indirectly in a c-C_4F_8 plasma by dissociative electron impact with its C_2F_4 by-product [3,4]. It is also known that both c-C_4F_8 and its by-product C_2F_4 molecules are widely used as base substrates for the formation of multilayer connections with low dielectric constants [5]. These molecules have a long lifetime in the atmosphere, of ~3200 years, which accounts for its high global warming potential. Nevertheless, despite the usefulness of this gas to the plasma etching industry, and other fields, there have not been enough studies carried out to understand its scattering properties. Therefore we took interest in carrying out investigations of both electron impact [total cross sections (TCSs) and differential cross sections (DCSs)] and positron impact total cross sections with these molecules to provide a data set that could be useful in understanding the basic physics and applications of these molecules. Though the electron cross sections are the ones needed for these various applications, the comparative study with positron cross sections aids in even better understanding of the electron cross sections themselves.

Although earlier measurements for TCSs exist in literature by Sanabia *et al.* [6] and Nishimura [7], there are large discrepancies between the two so that we decided to undertake this project using an independent method to investigate the TCSs for these important molecules. Other relevant earlier studies concentrated on electron scattering and include the derivative electron transmission experiments by Harland and Franklin [8], experimental ionization cross sections by Toyoda *et al.* [9] and Jiao *et al.* [10], and experimental and theoretical DCSs by Okamoto *et al.* [11] and Winstead *et al.* [12], respectively. The most recent studies among these pioneering works though are measurements of electron attachment, detachment, and electron affinity on c-C_4F_8 by Miller *et al.* [13], and the experimental differential cross sections for electron scattering from these molecules by Jelisavcic *et al.* [14].

Christophorou and Olthoff [3] gathered most of the studies carried out to date and compiled sets of recommended cross sections for the various scattering processes for these molecules using some averaging and extrapolation procedures, based on the available limited experimental and theoretical results. However, as they also point out, joint experimental and theoretical studies are awaited from different laboratories to enable compilation of accurate cross sections data for these molecules. We hope that the joint total cross sections (TCS) and integrated cross sections (ICS) results presented here should also go a long way towards offering a reliable basis set of data for better "recommended total cross sections" [3]. Electron diffraction (e.g., Ref. [15]) and infrared (e.g., Ref. [16]) studies have been used to establish the electronic and spectroscopic properties of these molecules, which also provide useful information for better understanding of some of the structures observed in our cross sections.

II. EXPERIMENTAL PROCEDURE

A. Total cross sections

The absolute TCSs for electron and positron scattering from these molecules have been measured for the energy range 0.7–600 eV using a linear transmission retarding po-

tential time-of-flight (RP-TOF) method in an apparatus setup similar to our previous measurements [17]. Only some specific features of the experiment are summarized here. A ^{22}Na radioisotope with an activity of ~ 80 μCi was used for the positron source. In order to obtain slow positron beams, a set of seven-overlapping tungsten mesh baked at 2100 °C was used as the moderator. The energy width of this beam is ~ 2 eV [full width at half maximum (FWHM)]. The slow electron beam, with an energy width of ~ 1 eV (FWHM), is composed of secondary electrons produced via multiple scattering from the same tungsten moderator. It must be pointed out though that this beam energy width is different from energy resolution of the RP-TOF experimental apparatus, which enables discussions of structures observed even below 1 eV [18]. The TCS values Q_m were derived from the equation

$$Q_m = -\frac{1}{nl}\ln\left(\frac{I_g}{I_v}\right), \tag{1}$$

where I_g and I_v refer to the projectile beam intensities transmitted through the collision cell with and without the target gas of number density n, respectively. l refers to the effective length of the collision cell and was established by normalizing our measured positron-N_2 TCSs to those of the positron-N_2 data of Hoffman *et al.* [19]. In this procedure, the value of l from the measurement just before the current positron-N_2 was assumed correct and used for the determination of the first values of the N_2 TCSs from the measured spectra over the randomly chosen 14–200-eV range. Ratios of the Hoffman *et al.* TCSs to our so-measured TCSs were then calculated over all the energy points of overlap, with each ratio value falling within the range $1 \pm 10\%$, and their average F was found. This value of F was then multiplied to the assumed l value to get the new effective cell length. This new value of l also makes sure that any instability of the pressure gauge that might have affected correct reading of the pressure values was accounted for. The cyclo-C_4F_8 TCSs presented here were confirmed to be pressure-independent in the present energy range by independent test experiments, which is an important aspect of measurements using a collision cell in the transmission RP-TOF setup [20]. The energy calibration was done using positron-N_2 TOF spectra measured at 20 energies in the randomly chosen region of 8–150 eV [21].

Our present apparatus setup has specifically been designed to have a collision cell with wide entrance and exit apertures for the weak positron beam intensities, i.e., for positron scattering experiments. As a result the ceratron detector detects some projectiles scattered through small angles. In order to derive accurate TCSs, it is necessary to account for this effect. For this, we take into account the collision cell geometry, the external magnetic field and the DCS data from experimental or theoretical results on the molecule being studied. The procedure for this has been described in detail previously [17,22]. The DCS data used for the correction for these molecules are those being jointly presented in this paper and those of Winstead and McKoy [12]. The relationship between the corrected TCS value (Q_t) and the measured value (Q_m) is given by

$$Q_t = Q_m + Q_f, \tag{2}$$

where Q_f is the cross section due to forward scattering. The forward scattering cross section Q_f is given by the equation

$$I_f = \frac{1}{\pi R^2 Q_t}\int_0^{\ell} dI(x)\int_0^{R} 2\pi\, r dr \times \int_0^{\theta_{\max}} \Phi(\theta,r,x,E,B) q(\theta)\sin\theta\, d\theta, \tag{3}$$

where $q(\theta)$ is the differential cross section (DCS), R is the diameter of the aperture of the collision cell, and B is the magnetic field. $dI(x)$ is the scattered intensity between x and $x+dx$, where x is the position coordinate parallel to the flight path and r the radial position coordinate. The function Φ is the transmission function and is a function of B (magnetic-field intensity), E (beam energy), r, x, R, and the effective collision cell length l. Thus, in the correction process, electron and positron TCSs are treated separately using their respective magnetic fields of 4.5 and 9 G, respectively. For this paper, the correction for electron TCSs amounts to less than 4% below 10 eV, an average 4.5% at 10–30 eV, and becomes less than 1% above 100 eV. Because there is no DCS data available for positron scattering, the same electron DCS data were used for an attempt on the correction of positron TCSs too. This correction for positron scattering amounted to $\sim 10\%$ at 0.7 eV, decreased to 2% with increasing energy up to 7 eV, an average 10% at 8–30 eV, and then continued to decrease with increasing energy until it became $\sim 1\%$ at 600 eV. From our experience, these correction rates for positron TCSs, using electron DCSs, could be a few percent less than rates obtained using the actual positron DCSs, and thus positron DCSs are needed for a better correction for this forward scattering effect. However, for positron TCSs, any such inadequacy in the forward scattering correction, if at all, does not affect the type of structures we observe in the TCSs, and thus our results and the discussions presented here are credible and useful for applications.

The errors shown in the data in Table I are the total uncertainties made up of contributions from errors due to beam intensities, estimation of the effective cell length, and fluctuations in the gas density during measurements. This sum of all the uncertainties was estimated to be 5.2–6.3 % for electron and 6.4–9.7 % for positron impact. These uncertainties are made up of contributions from the $<1.3\%$ and $<4.6\%$ beam intensities ($\Delta I/I$) for electron and positron impact, respectively, where I refers to $\ln(I_g/I_v)$ in Eq. (1), the contribution from the gas density, $\Delta n/n$, which was $<3\%$ for these target molecules, and that due to the determination of the effective length of the collision cell $\Delta l/l$, which was about 2%.

B. Differential cross sections

The apparatus used in the present DCS measurements is the same as that used in previous studies [23]. The impact

TABLE I. Perfluorocyclobutane (c-C_4F_8) positron and electron TCSs (10^{-16} cm^2).

Energy (eV)	Positron	Electron	Energy (eV)	Positron	Electron
0.7	11.9±1.1		11	22.7±1.8	37.9±2.1
0.8		22.9±1.4	12	21.9±1.8	37.3±2.1
1.0	13.6±1.1	22.2±1.3	13	23.6±1.9	38.4±2.2
1.2		21.7±1.2	14	23.4±1.8	37.6±2.2
1.3	14.7±1.1		15	26.0±2.0	39.0±2.2
1.4		20.4±1.2	16	24.7±1.9	39.0±2.3
1.6	15.8±1.2	19.9±1.2	17	25.5±2.0	39.6±2.2
1.8		19.4±1.2	18	25.8±2.1	39.3±2.3
1.9	16.6±1.2		19	26.1±2.1	40.2±2.3
2.0		18.9±1.2	20	25.1±2.3	39.8±2.3
2.2	16.8±1.2	18.7±1.1	22	26.1±2.1	39.5±2.2
2.5	17.3±1.2	19.7±1.2	25	26.0±1.8	40.0±2.3
2.8	17.9±1.3	20.1±1.2	30	26.2±1.8	39.8±2.3
3.1	17.4±1.2	21.2±1.2	35		40.6±2.4
3.4	17.6±1.3	21.9±1.3	40	26.9±1.8	40.4±2.3
3.7	18.1±1.3	23.9±1.4	50	25.2±1.7	38.2±2.2
4.0	17.6±1.2	24.5±1.4	60	25.2±1.7	36.4±2.1
4.5	19.1±1.3	27.9±1.6	70	24.8±1.7	35.3±2.0
5.0	20.1±1.4	30.0±1.7	80	25.1±1.7	33.5±1.9
5.5	20.9±1.4	31.0±1.8	90	23.6±1.6	32.4±1.9
6.0	21.5±1.5	32.0±1.9	100	24.1±1.6	31.3±1.8
6.5	21.4±1.5	34.9±2.0	120	23.1±1.6	29.6±1.7
7.0	21.3±1.5	35.0±2.1	150	22.1±1.5	27.0±1.6
7.5	22.8±1.5	37.4±2.1	200	20.4±1.4	23.7±1.3
8.0	23.2±1.6	37.6±2.2	250	18.7±1.3	21.0±1.2
8.5	22.6±1.6	39.1±2.2	300	17.4±1.2	19.7±1.1
9.0	23.5±1.8	38.5±2.3	400	15.6±1.1	16.9±1.0
9.5	22.5±1.8	38.2±2.3	500	13.6±1.0	14.9±0.8
10	23.3±1.7	37.2±2.2	600	12.4±0.8	13.3±0.7

energies were from 1.5 to 100 eV in the present measurements and the absolute cross sections were obtained by the relative flow technique [24] using helium as the reference gas. All the other experimental details pertaining to the measurements of c-C_4F_8 DCSs can be found in Ref. [14].

The DCSs were analyzed using a molecular phase-shift approach [25] in order to extrapolate the DCSs to lower and higher angles, i.e., $\theta < 20°$ and $\theta > 130°$, to facilitate derivation of the integral cross sections (ICS). Briefly, the fitting formulas can be described in an expansion as

$$d\sigma(\theta)/d\Omega = |f(\theta)|^2,$$

$$2ikf(\theta) = N(k)\{\Sigma[S_l(k) - 1](2l + 1)P_l(\cos\theta) + C_L(\theta)\},$$

$$C_L(\theta) = 2i\pi\alpha k^2[1/3 - 1/2(\theta/2) - \Sigma P_l(\cos\theta)/(2l + 3)(2l - 1)],$$

where $C_L(\theta)$ is the Born approximation for the higher phases in the Thompson form [26], k is the wave number of the electron, α the atomic/molecular polarizability, $P_l(\cos\theta)$ are the Legendre polynominals, and $f(\theta)$ is the scattering amplitude. The χ^2 approximations were applied to get the reliable fittings. Overall experimental errors in the DCSs were estimated to be 15–20 %.

III. RESULTS AND DISCUSSION

The numerical values for both electron and positron TCSs are shown in Table I, together with the associated uncertainties derived as explained above. A preliminary discussion of the electron TCSs presented here has been published elsewhere [27]. However, the current data presents an improved data set because of the forward scattering correction that became possible because using the just measured DCSs. The electron DCSs used for the discussions here have already been submitted elsewhere for publication [14] and so data tables and graphs are not reproduced in this paper. However, an independent partial wave analysis method has been used to evaluate integrated cross sections (ICS) from these DCSs, i.e., giving a result a few percent different from the data of

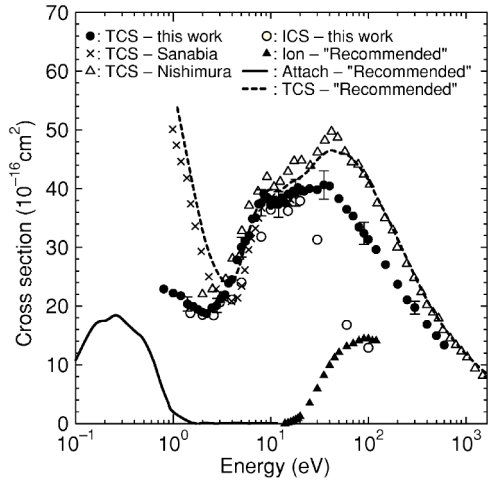

FIG. 1. c-C_4F_8 electron scattering: (●) present TCS; (○) present ICS; (×) Sanabia *et al.* [5] TCS; (△) Nishimura [6] TCS; (----), (—), and (▲) Christophorou and Olthoff [3] recommended TCS, attachment, and ionization cross sections.

Ref. [14], and thus the current ICS result is shown in Fig. 1 and used for the discussions in this paper.

A. Electron impact

The present total cross section (TCS) results are shown in Fig. 1, together with the present integrated cross sections (ICS), the other two experimental TCSs by Sanabia *et al.* [6] and Nishimura [7], and the Christophorou and Olthoff [3] recommended TCS, attachment, and ionization cross sections. The recommended TCSs have been obtained by carrying out a least-squares averaging of the Sanabia *et al.* and Nishimura data in the region of overlap, and extrapolating the data using some fitting function to higher and lower energies by normalizing the results to the Sanabia *et al.* data ($\leqslant$4 eV) and to the Nishimura data ($\geqslant$20 eV) [3]. As such, the recommended TCS basically reflects on the Sanabia *et al.* and Nishimura data and so is not used for the discussions that follow. There are a number of interesting features observed from these data, which are summarized as follows. (i) Below 2 eV, TCSs for c-C_4F_8 continue to increase without showing any sign of a slowing down to any peak. This behavior of c-C_4F_8 electron TCSs agrees with the electron attachment rates studies, below 1 eV, which have been found to rise steeply as the electron energy approaches 0 eV [3,28,29]. Miller *et al.* [13,30] have also estimated an electron affinity of +0.63 eV, for these molecules, from electron attachment experiments, and suggested that this phenomenon could in fact be corresponding to electron capture into the lowest unoccupied molecular orbital (LUMO). (ii) At 2.2 eV, c-C_4F_8 TCSs show a minimum which Sanabia *et al.* also observed, albeit at 3.5 eV, and suggested it to be a Ramsauer-Townsend minimum. Theoretical studies are awaited though to confirm the exact origin and nature of this minimum. (iii) Though c-C_4F_8 derivative electron transmission experiments have suggested a resonance peak at 5.8 eV [31], this is not observed in our TCSs, possibly because its cross section is smaller than would be observed in our TCSs which are more than 35×10^{-16} cm^2 at this energy range. (iv) The peak at $\sim$8.5 eV corresponds well with studies of dissociative electron attachment, i.e., with the production of the F^-, F_2^-, and CF_2^- ions [3], and thus should be suggesting the existence of negative ion states. (vi) Beyond 40 eV, these TCSs show a monotonously decreasing trend.

On the comparison between the current TCS and ICS results, fairly good qualitative and quantitative agreement is observed between the TCS and ICS results below 10 eV. This agreement, in terms of the observed structures and their positions between the TCS and ICS is consistent with the physics that, in this region below the ionization threshold, elastic scattering is the dominant channel. In the region below 10 eV, the next significant channel is electron attachment which, however, remains below 1 Å^2 until below 1 eV. The ICS also reproduces the shallow valley observed in the TCS between 9 and 20 eV. The decrease in the ICS values above 20 eV is consistent with the trend shown by the ionization cross sections, which are gradually rising so that the peak appearing at about 40 eV, in the TCSs, should be consisting of strong contributions from the ionization channel. However, that the ionization cross section, though peaking at about 100 eV, is only about 40% of the present TCS, and that the electron attachment contribution to the TCS below 1 eV is large, are properties that would make this gas a possible candidate for gaseous dielectric applications, i.e., properties that enables the gas to keep the number of free electrons low. The same DCS experimental setup was used to carry out measurements of the energy dependence of the dominant vibrational excitation feature that was observed at an energy loss of 0.16 eV [14], in the energy range 1.5–20 eV. The spectrum shows a large peak at 7.5 eV, enhancements at 4.9 and 11 eV, and rising cross sections below 3 eV. The 7.5-eV structure is attributable to the ^2E and $^2A_2$ resonances theoretically predicted by Winstead *et al.* [12]. The remaining three features have been associated with negative ion resonances at these energies. It is noted here that though the 7.5-eV resonance peak fairly coincides with the $\sim$8.5-eV peak feature observed in the TCS, its direct contribution is very minimal considering that its cross section is only $\sim0.2\times10^{-16}$ cm^2, compared to the TCS which is $\sim39\times10^{-16}$ cm^2 in this region. The same applies to the other above-mentioned three features observed in the energy-loss spectrum.

Comparison of our c-C_4F_8 TCSs with other data, Fig. 1, shows a generally good qualitative agreement with both Sanabia *et al.* [6] and Nishimura [7] TCSs. However, quantitative differences are observed below 3 eV, where our data is comparable with the Nishimura data but becoming almost half the magnitudes of the Sanabia *et al.* data. A comment is warranted on this significant difference between the sharply rising Sanabia *et al.* TCS (below 3 eV) and our gradually rising result (below 2 eV). As pointed out above, an analysis of the scattering channels open at such low energies for these molecules, e.g., below 5 eV, shows that after the elastic channel, the next significant contribution to the TCS comes from electron attachment [3]. However, as shown in Fig. 1, the electron attachment cross section remains $<0.05\times10^{-16}$ cm^2 at all energies $\geqslant$2 eV and rises only to 1.97×10^{-16} cm^2 at 1 eV. Based on the analysis that at these energies the TCS is almost made of the sum of the elastic (i.e.,

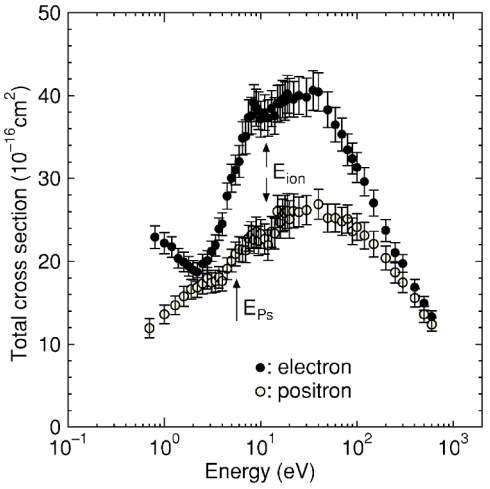

FIG. 2. Present c-C_4F_8 electron (●) and positron (○) scattering TCSs.

the present ICS is in fact made up of elastic and rotational excitation) and attachment cross sections, and with the contribution from vibrational excitation being so small [3], the sharp rise observed in the Sanabia *et al.* cannot be accounted for.

Besides, our TCS result shows a minimum centered at 2.2 eV, seemingly in better agreement with the ICS data, compared to that of Sanabia *et al.* at 3.5 eV. In the 10–100-eV peak region, there is general agreement with the Sanabia *et al.* data though the Nishimura data are larger by about 23%. This difference between our result and the Nishimura data above 10 eV warrants attention as well. Though we cannot be exact in analyzing the origin of this difference, we carried out a very rough inspection of the Nishimura and our TCS in this energy region using the ionization and ICS data shown in Fig. 1, though this analysis should rather be more reliable in the energy range above a few tens of eV. Above the ionization threshold, to a rough extent, the sum of the ICS and the ionization cross section should constitute more than 75% of the total cross section, with the difference coming from the other minor channels, including electronic and vibrational excitations, dissociation, and other channels. See Ref. [3] for the numerical values of the cross sections of these minor channels. In view of this, the differences between the sum of the ICS and the ionization cross section are found to be 7.5% (18.3%), 1.8% (14.5%), 6.9% (24.1%), 21.7% (54.8%), and 14.7% (49.7%) at 15, 20, 30, 60, and 100 eV, respectively, for our (Nishimura) data. Based on this analysis, we surely feel that the Nishimura data above 30 eV may be too high to be physically reasonable.

Beyond 40 eV, however, both our TCSs and the Nishimura TCSs show the same monotonically decreasing trend.

B. Positron impact

Figure 2 shows the present positron and electron TCSs for these molecules. Unfortunately, to our knowledge, there are neither experimental nor theoretical positron scattering cross sections for comparison with our data, which makes the analysis carried out here rather speculative, as it awaits ionization, elastic, various excitation, and other partial cross studies for better understanding of the nature and origin of the features observed. The positron TCSs show a gradually increasing rather smooth energy dependence from 0.7 eV towards the broad peak spanning from about 8 to 120 eV. However, non-negligible minor shoulders are observed in the vicinity of 3 and 9 eV, and the valley at ~12 eV. The unpronounced shoulder at about 3 eV, if real, lies below positronium (Ps) formation threshold, E_{Ps}, i.e., 5.4 eV, and surely needs to be carefully examined to know its origin. However, speculation based on the known physics enables us to suspect that it should be due to rovibrational excitation. The hump at ~9 eV should be made up of contributions from Ps formation and electronic excitation. It is not clear what cause of the valley at ~12 eV could be. Contrarily, it could be that the physics to be learned is not from the valley itself but the TCS enhancement that follows above this energy, which would be attributable to impact ionization, i.e., which has a threshold at 12.2 eV. However, as energies increase above this peak region, the TCSs decrease rather monotonically towards 600 eV, in the limit of experimental errors.

C. Electron and positron impact: A comparative study

The electron and positron data for these molecules are shown in Fig. 2. At energies below 2.2 eV, electron and positron TCSs are found to show opposite trends, i.e., a rising trend for electron impact in contrast to a decreasing trend for positron impact. This observation of contrasting TCS behavior between electron and positron impact with respect to decreasing incident energy could be either solely due to the rising electron attachment cross section (see Fig. 1), or with some contribution from the delicate balance between the attractive and repulsive interactions resulting in a virtual state for electron impact hence causing an increase in electron TCSs, while the near-zero scattering for positron impact causes a drop in positron TCSs [18]. Above 2 eV, electron TCSs are seen rapidly rising compared to positron TCSs that are rather slowly rising towards the peak plateau, albeit with an unpronounced minimum at about 12 eV that incidentally coincides with that in the electron TCSs at 10–13 eV. The difference between these electron and positron TCSs continues to increase until the electron main resonance peak at about 7–70 eV, which itself consists of three peaks at ~8.5, 18, and 40 eV. Because of the dominant contribution from shape resonances in this peak region, electron TCSs are greater than the corresponding positron TCSs by up to 60%. These electron and positron TCSs tend towards merging above 120 eV. This should be because at these higher energies, only the long-range interaction dominates the scattering event and as a result only the first Born term is sufficient for describing the scattering where the square of the charge of the incoming particle comes into the cross-section formula leading to this convergence phenomenon in electron and positron TCSs, i.e., since these two projectiles only differ in the sign of their charges.

IV. CONCLUSIONS

TCSs have been experimentally investigated for c-C_4F_8 collisions with 0.8–600 eV electrons and 0.7–600 positrons.

Rising TCSs below 2 eV due to increasing electron attachment cross sections towards 0 eV have been observed. Another peak has also been observed at ~8.5 eV and attributed to dissociative electron attachment with the production of F^-, F_2^-, and CF_2^- ions. Consistence has been observed between the electron TCS, ICS, attachment, and ionization cross sections. However, though general qualitative agreement has been observed between our TCS and the other two TCS data sets, significant quantitative differences have been observed below 3 eV and above 10 eV. An interesting difference in the low-energy TCSs between electron and positron impacts is observed below 2 eV, i.e., an increasing trend for electron-TCSs versus a gradual drop for positron TCSs. This difference has been attributed to the bound states resonances observed in electron scattering but not found in the positron counterpart. The two TCSs tend toward merging above 600 eV. This should be because at these higher energies, only the first Born term dominates the scattering event.

ACKNOWLEDGMENTS

The work was supported in part by the Ministry of Education, Sport, Culture and Technology and the Japan Society for Promotion of Science (JSPS) and the Collaborative Research Grant by the National Institute for Fusion Science. C.M. is also grateful to the JSPS for financial support under Grant No. P04064, and also to Yamaguchi University as he did part of this work while he was a Ph.D. student there.

[1] S. Samukawa and T. Mukai, in *Proceedings of the International Symposium on Electron-Molecule Collisions and Swarms*, edited by Y. Hatano, H. Tanaka, and N. Kauchi, Tokyo, Japan, 18–20 July 1999, p. 76.
[2] H. Kimura, K. Shiozawa, K. Kawai, H. Miyatake, and M. Yoneda, Jpn. J. Appl. Phys., Part 1 **34**, 2114 (1995).
[3] L. G. Christophorou and J. K. Olthoff, J. Phys. Chem. Ref. Data **30**, 449 (2001).
[4] J. N. Butler, J. Am. Chem. Soc. **84**, 1393 (1962).
[5] R. Panajotovic, M. Jelisavcic, R. Kajita, T. Tanaka, M. Kitajima, H. Cho, H. Tanaka, and S. J. Buckman, J. Chem. Phys. **121**, 4559 (2004).
[6] J. E. Sanabia, G. D. Cooper, J. A. Tossell, and J. H. Moore, J. Chem. Phys. **108**, 389 (1998).
[7] H. Nishimura, in *Proceedings of the International Symposium on Electron-Molecule Collisions and Swarms* (Ref. [1]), p. 103.
[8] P. W. Harland and J. L. Franklin, J. Chem. Phys. **61**, 1621 (1974).
[9] H. Toyoda, M. Iio, and H. Sugai, Jpn. J. Appl. Phys., Part 1 **36**, 3730 (1997).
[10] C. Q. Jiao, A. Garscadden, and P. D. Haaland, Chem. Phys. Lett. **297**, 121 (1998).
[11] M. Okamoto, M. Hoshino, Y. Sakamoto, S. Watanabe, M. Kitajima, H. Tanaka, and M. Kimura, in *Proceedings of the International Symposium on Electron-Molecule Collisions and Swarms* (Ref. [1]), p. 191.
[12] C. Winstead and V. McKoy, J. Chem. Phys. **114**, 7407 (2001).
[13] T. M. Miller, J. F. Friedman, and A. A. Viggiano, J. Chem. Phys. **120**, 7024 (2004).
[14] M. Jelisavic, R. Panajotovic, M. Kitajima, M. Hoshino, H. Tanaka, and S. J. Buckman, J. Chem. Phys. **121**, 5272 (2004).
[15] H. P. Lemaire and R. L. Livingston, J. Am. Chem. Soc. **74**, 5732 (1952).
[16] R. P. Bauman and B. J. Bulkin, J. Chem. Phys. **45**, 496 (1966).
[17] O. Sueoka, S. Mori, and A. Hamada, J. Phys. B **27**, 1452 (1994).
[18] M. Kimura, C. Makochekanwa, and O. Sueoka, J. Phys. B **37**, 1461 (2004).
[19] K. R. Hoffman, M. S. Dababneh, Y. F. Hsieh, W. E. Kauppila, V. Pol, J. H. Smart, and T. S. Stein, Phys. Rev. A **25**, 1393 (1982).
[20] R. E. Kennerly and R. A. Bonham, Phys. Rev. A **17**, 1844 (1978).
[21] O. Sueoka and S. Mori, J. Phys. B **19**, 4035 (1986).
[22] O. Sueoka, C. Makochekanwa, and H. Kawate, Nucl. Instrum. Methods Phys. Res. B **192**, 206 (2002).
[23] H. Tanaka, T. Ishikawa, T. Masai, T. Sagara, L. Boesten, M. Takekawa, Y. Itikawa, and M. Kimura, Phys. Rev. A **57**, 1798 (1998).
[24] S. K. Srivastava, A. Chutjian, and S. Trajmar, J. Chem. Phys. **63**, 2659 (1975).
[25] R. Panajotovic, M. Kitajima, H. Tanaka, M. Jelisavic, J. Lower, L. Campbell, M. J. Brunger, and S. J. Buckman, J. Phys. B **36**, 1615 (2003).
[26] D. G. Thompson, Proc. R. Soc. London, Ser. A **294**, 160 (1966).
[27] C. Makochekanwa, M. Kimura, and O. Sueoka, *Gaseous Dielectrics X*, edited by Loucas G. Christophorou, James K. Olthoff, and Panayota Vassiliou (Springer, New York 2004), p. 181.
[28] A. A. Christodoulides, L. G. Christophorou, R. Y. Pai, and C. M. Tung, J. Chem. Phys. **70**, 1156 (1979).
[29] A. Chutjian and S. H. Alajajian, J. Phys. B **20**, 839 (1987).
[30] T. M. Miller, R. A. Morris, A. E. S. Miller, A. A. Viggiano, and J. F. Paulson, Int. J. Mass Spectrom. Ion Processes **135**, 195 (1994).
[31] I. Ishii, R. McLaren, A. P. Hitchcock, K. D. Jordan, Y. Choi, and M. B. Robin, Can. J. Chem. **66**, 2104 (1988).